

Multimorphological Self-Assemblies of Amphiphilic Graft Polyphosphazenes with Oligopoly(*N*-isopropylacrylamide) and Ethyl 4-Aminobenzoate as Side Groups

Jian Xiang Zhang,^{†,‡} Li Yan Qiu,^{*,†} Yi Jin,[†] and Kang Jie Zhu[‡]

College of Pharmaceutical Sciences, Zhejiang University, Hangzhou 310031, China, and Institute of Polymer Science, Zhejiang University, Hangzhou 310027, China

Received October 4, 2005

Revised Manuscript Received October 14, 2005

Introduction

Polymeric aggregates self-assembled from amphiphilic block copolymers have received increasing attention in the past few years. A variety of aggregate structures, including spherical micelles, rodlike micelles, vesicles, or lamellae, can be self-assembled from block copolymer at the mesoscopic level.¹ Compared to supramolecular aggregates based on low molecular amphiphiles, polymeric self-assemblies not only exhibit the advantage of superior stability and toughness,² but also offer numerous possibilities to tailor physicochemical and biological properties by varying block length and chemical structure and conjugating with biomolecules. This makes copolymer assemblies highly interesting as transfection vectors,³ protective shells for sensitive enzymes,⁴ drug delivery systems,⁵ or as microreactors where chemical reactions can be performed at the molecular level.⁶ In addition to block copolymers,⁷ giant vesicle formation through self-assembly of complementary random copolymer was reported by Ilhan et al.⁸ Furthermore, generation-dependent aggregation and molecular self-assembly were also observed for dendrimers, hyperbranched copolymers and dendrigraft copolymers.⁹ However, few researchers have focused the study on self-assembly behaviors of graft copolymers, particularly those of the same series of copolymers in various aqueous solutions. Our attention has been concentrating on the preparation and potential application of graft polyphosphazenes and their assemblies. In this paper, we report the assembly morphologies of amphiphilic graft polyphosphazene containing oligopoly(*N*-isopropylacrylamide) and ethyl 4-aminobenzoate as co-side groups (PNIPAm/EAB-PPPs) with different hydrophobic/hydrophilic balance in aqueous solution.

Experimental Section

Materials. Amphiphilic graft copolymers PNIPAm/EAB-PPPs with different hydrophilic/hydrophobic balances were synthesized according to the literature.¹⁰ The physicochemical characteristics of copolymers were presented in Table 1.

Preparation of PNIPAm/EAB-PPP Aggregates. Since copolymers **1** and **2** are easily dissolved in water, their aggregates were obtained by directly dissolving the copolymer into distilled water (5 mg/mL). Supramolecular aggregates from copolymer **3**, on the other hand, were prepared by dialysis method. Briefly, 20 mg of copolymer **3** was dissolved in 2 mL of organic solvent, and the solution was dialyzed against distilled water using a dialysis membrane tube (MW cutoff

Table 1. Physicochemical Properties of PNIPAm and the Copolymers PNIPAm/EAB-PPPs

polymer	mole ratio ^a		<i>M</i> _n	<i>M</i> _w	LCST (°C)	CAC (g/L)	<i>K</i> _{SV} (M ⁻¹)
	PNIPAm <i>x</i>	EAB <i>y</i>					
PNIPAm			1900 ^b 1400 ^c	2200	33.8		
copolymer 1	1.80	0.20	22 000	43 000	32.6	0.037	2.0
copolymer 2	1.00	1.00	18 589	38 035	36.0	0.028	1.7
copolymer 3	0.68	1.32	12 344	21 215	35.0	0.015	0.9

^a *x* + *y* = 2.0. ^b Obtained by GPC. ^c Determined by elemental analysis.

3500) for 2 days at 15 °C. Organic solvents including DMF, dimethylacetamide (DMAc), DMSO, and THF were employed in this experiment. The outer solution was exchanged at appropriate intervals. All the sample solutions were diluted to a final copolymer concentration of 2.0 mg/mL, and these samples were used without further treatment for TEM characterization.

Morphology Observation. TEM images were obtained using a JEM 1230 operating at an acceleration voltage of 80 kV. Copper EM grids were coated with a thin film of Formar. Unless stated otherwise, all TEM samples were prepared at 15 °C by dipping a TEM grid into a copolymer solution, and the extra solution was blotted with filter paper. To observe the internal morphology of the aggregates derived from DMAc and DMSO, a powder sample of nanoparticles was embedded in epoxy resin, and thin sections of ~150 nm in thickness were obtained by microtoming the resin sample at room temperature.

Samples for AFM were prepared by coating aqueous copolymer solution onto freshly cleaved mica. AFM images were obtained using a Nanoscope III microscope (Digital Instruments) in the tapping mode with a silicon cantilever.

Fluorescence Measurements. The quenching of pyrene solubilized in copolymeric aggregates by I⁻ (KI) was also investigated. NaCl was used to keep the ionic strength constant.¹¹ A small amount of S₂O₃²⁻ (ca. 10⁻⁴ M) was added to prevent oxidation of I⁻ into I₃⁻. The solutions were equilibrated at 10 °C before the measurements. Polymer concentration was 1 mg/mL. For copolymer **3**, the sample was prepared using THF as solvent in the dialysis procedure.

Results and Discussion

The chemical structure of amphiphilic graft copolymers PNIPAm/EAB-PPPs was illustrated by Figure 1, and their physicochemical properties were presented in Table 1.

Eisenberg and co-workers have studied multimorphological self-assemblies of block copolymers in detail.¹² However, few systematic researches have been focused on aggregates produced by graft copolymers. TEM and AFM were applied to offer the information about the morphologies of copolymer aggregates in this study. As shown in Figure 2a, physically cross-linked network

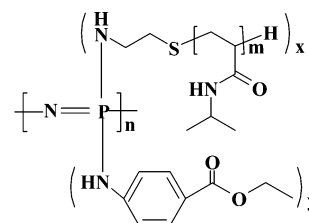


Figure 1. Chemical structure of amphiphilic graft copolymer PNIPAm/EAB-PPPs.

[†] College of Pharmaceutical Sciences, Zhejiang University.

[‡] Institute of Polymer Science, Zhejiang University.

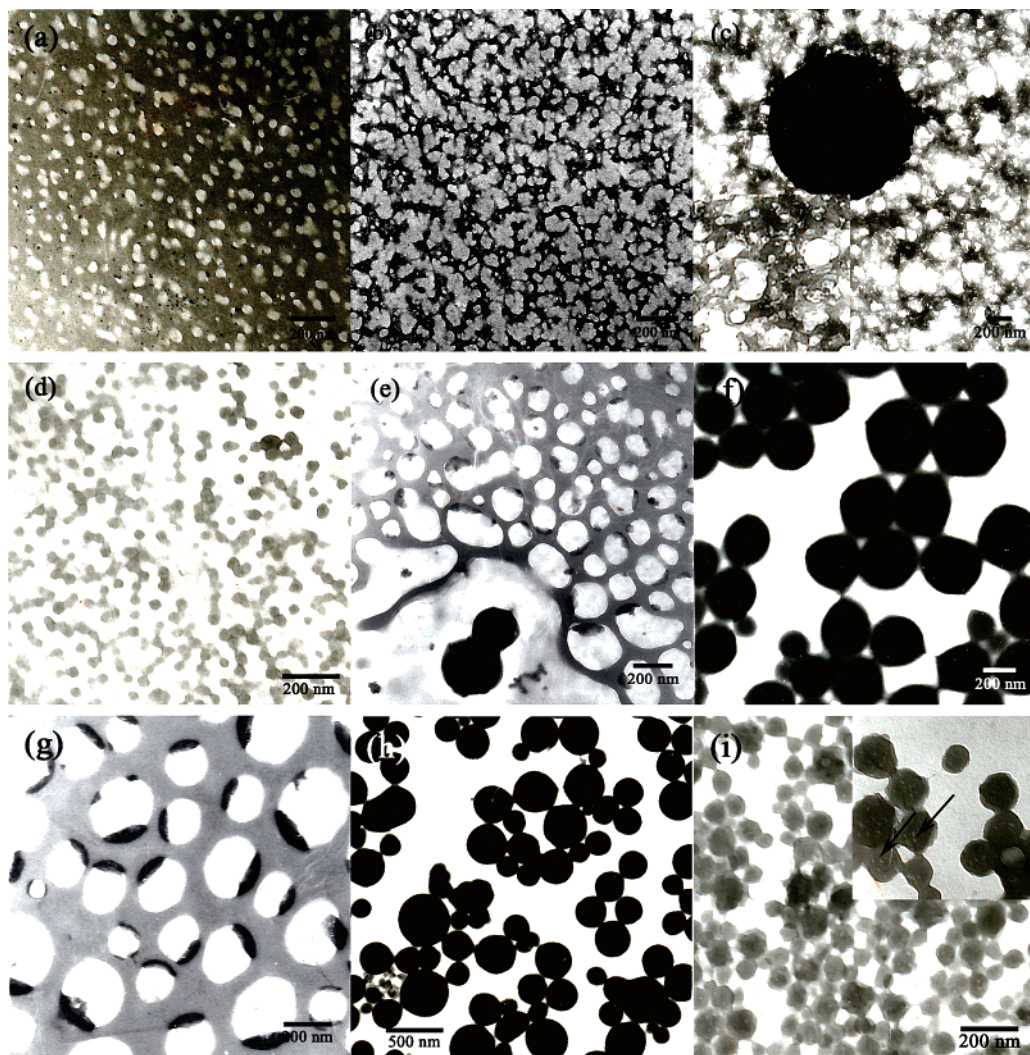


Figure 2. TEM images of aggregates made from amphiphilic copolymers (a) copolymer 1, 5 mg/mL; (b) copolymer 1, 2 mg/mL; (c) copolymer 2, 5 mg/mL; (d) copolymer 3, DMF as solvent; (e) copolymer 3, DMAc as solvent; (f) copolymer 3, DMAc as solvent, cutoff aggregates after being filtered through a $0.22\ \mu\text{m}$ microporous membrane; (g) copolymer 3, DMAc as solvent, filtrate after being filtered through a $0.22\ \mu\text{m}$ microporous membrane; (h) copolymer 3, DMSO as solvent; (i) copolymer 3, THF as solvent.

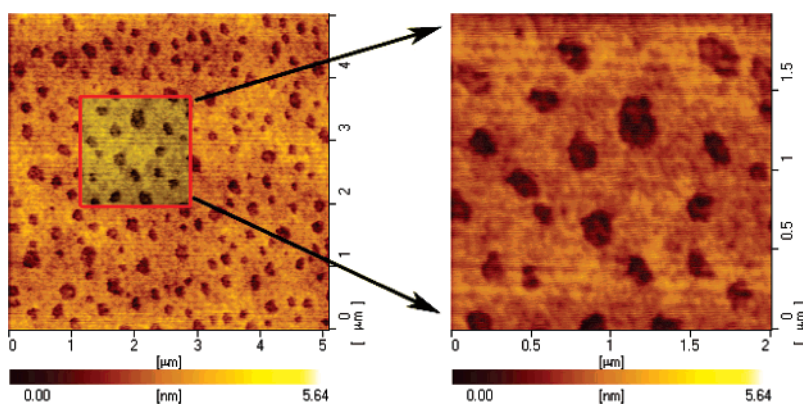


Figure 3. AFM images of assemblies from copolymer 1 (5 mg/mL). The sample was prepared at $15\ ^\circ\text{C}$.

aggregates were observed for copolymer 1, which were produced by dissolving the polymer into an aqueous solution. Similar morphology was also observed by AFM (Figure 3). In addition, as the copolymer concentration was diluted from 5 to 2 mg/mL, a “loose” network structure originated from partial dissociation of copolymer chains was formed (Figure 2b), since this aggregate was kinetically instable. For the copolymer 2, however, sphere-shaped and network structure aggregates co-

existed (Figure 2c). Interestingly, copolymer 3 based aggregates exhibited solvent-dependent morphologies. When DMF was employed as an organic solvent in dialysis procedure, nanospheres in an average diameter of 50 nm with a low polydispersity were obtained (Figure 2d). This micelle-like aggregate of spherical geometry has been identified in many studies on both block and graft copolymers.¹³ As DMAc was employed, however, both spherical nanoparticles and network

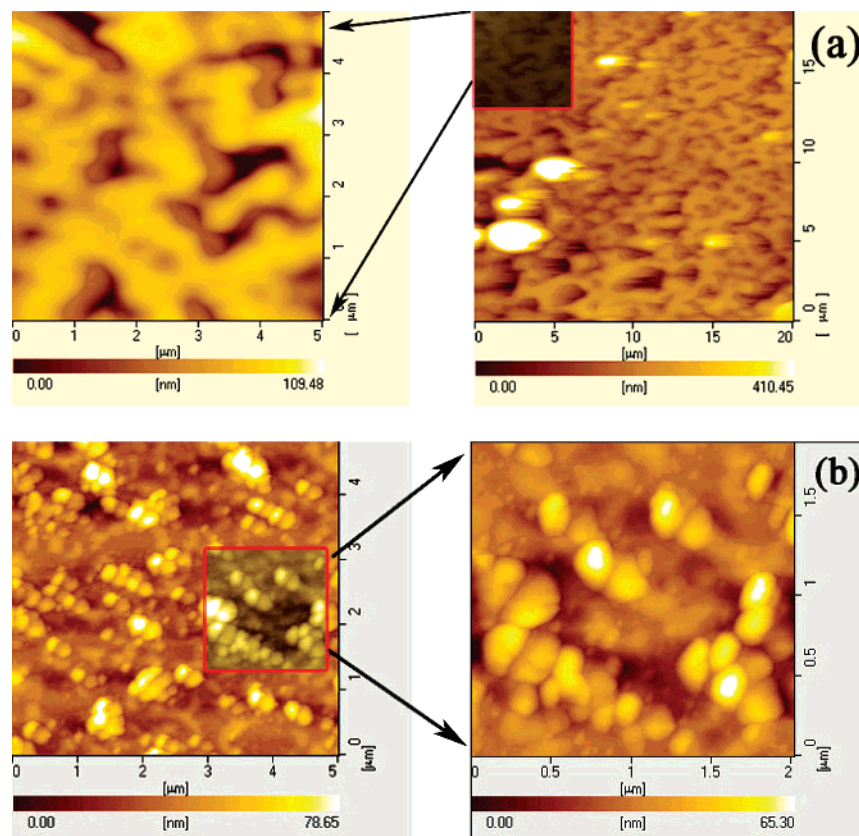


Figure 4. AFM images of aggregates based on copolymer **3**. The samples were prepared using DMAc at (a) 15 °C and (b) 50 °C, respectively.

micelles were observed shown in Figure 2e. More clearly, after this aggregate solution was filtered through 0.22 μm microporous membrane, the cutoff aggregates were nanoparticles while self-assemblies remaining in the filtrate displayed network morphology (Figure 2, parts f and g). The network structure was also confirmed by AFM as shown in Figure 4a. In the case of DMSO, well-defined microspheres were produced as presented in Figure 2h. In addition, high-genus nanoparticles were obtained as THF was employed as an organic solvent, which seems a new morphology for graft copolymers assemblies (Figure 2i).^{2b,14}

In the case of amphiphilic graft polyphosphazenes, the type of hydrophobic side group and copolymer composition significantly influenced multiple morphology formation. When another amphiphilic graft polyphosphazene PNIPAm/GlyEt-PPP (ethyl glycinate (GlyEt) as hydrophobic groups) was studied previously, it was found that the self-assemblies' morphology was not related to the solvent used for dialysis, but would change from nanoparticles to network upon the GlyEt content decreased.¹⁵ This effect of copolymer composition on multimorphology formation was also demonstrated for PNIPAm/EAB-PPPs as clearly shown in TEM pictures in Figure 2. Network structure was assembled from the copolymers with low EAB content, while both network aggregates and sphere-shaped particles were observed for copolymer **2** with medium EAB content. In addition, the aggregate morphologies of copolymers **1** and **2** seem to be independent of preparation procedure. That is, as dialysis method was adopted, solvent type did not effect the assembly morphology. Interestingly, the aggregates of copolymer **3** containing higher EAB content exhibited versatile morphologies, which ranged from network, sphere to high-genus particles, depending on solvent

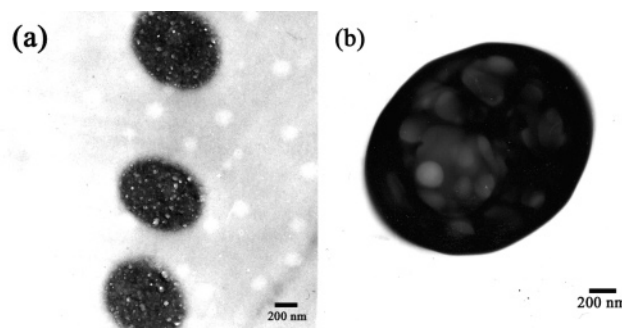


Figure 5. Internal morphology of the aggregates from copolymer **3** using various solvents (a) DMAc and (b) DMSO.

type employed in aggregates preparation procedure. Where the aggregates prepared using DMAc or DMSO are concerned, note should be taken that these large spheres also exhibited an internal network structure (Figure 5), which was similar to the aggregate morphology observed for the copolymer with low EAB content. Consequently, this type of large particles are different from that reported by Eisenberg and co-workers, since their large complex micelles were filled with bulk reverse micelles.¹⁶

Moreover, repulsive interactions among the corona chains may also be a main factor to dominate aggregate morphology. The corona chains of aggregates studied here were composed of PNIPAm, which is highly hydrated and exhibits an extended conformation at temperatures below its LCST, while dehydrates and therefore collapses at temperature near or above its LCST. Accordingly, corona chain repulsion varied concomitantly with temperature variation, which in turn led to the change in aggregate morphology. This was

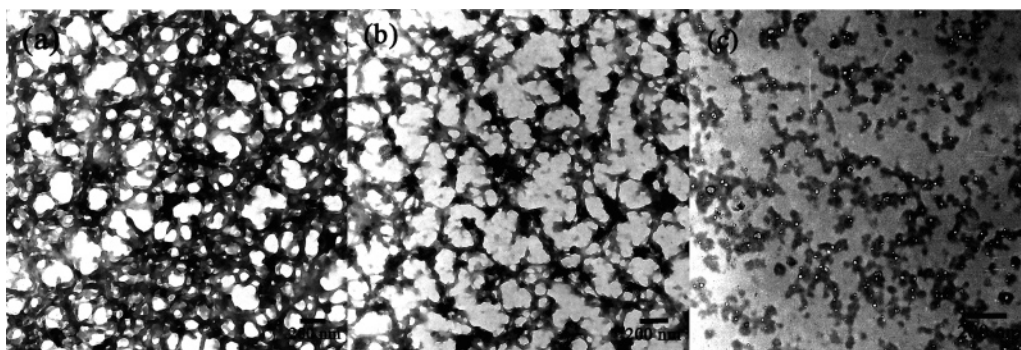


Figure 6. TEM images of aggregates from copolymer 1 at (a) 15, (b) 30, and (c) 50 °C. The polymer concentration was 4 mg/mL.

indeed the case. As shown in Figure 6, parts a and b, network aggregates of copolymer 1 were transformed into a loosely cross-linked structure, when the sample preparation temperature increased from 15 to 30 °C, and even nearly into particles for aggregates at about 50 °C (Figure 6c). This was consistent with our previous result, where sphere-shaped particles were observed for amphiphilic polyphosphazene with 92 mol % PNIPAm and 8% EAB once the temperature increased from 25 to 45 °C.¹⁰ Similarly, as illustrated in Figure 4 of AFM images of copolymer 3 based aggregates derived from DMAc, network morphology at 15 °C was transformed into sphere particles, which were obtained at 50 °C.

Further information regarding the nature of the polymeric aggregates was obtained by fluorescence quenching measurements of pyrene solubilized in the hydrophobic domains of the graft copolymers.¹⁷ I[−] was used as a quencher, which is negatively charged and highly hydrated and cannot access hydrophobic microdomains (e.g., micellar cores). Assuming a collisional quenching mechanism, the following equation describes the quenching process

$$F_0/F = 1 + K_{SV}[I^-]$$

where F and F_0 are the total fluorescence intensities of pyrene with and without I[−] respectively. K_{SV} is the Stern–Volmer quenching constant and is defined as

$$K_{SV} = k_q\tau_0$$

where k_q is the bimolecular rate constant and τ_0 is the fluorescence lifetime of pyrene in the absence of quencher.¹¹

The variation of fluorescence intensity with [I[−]] at constant ionic strength followed the Stern–Volmer formulation without change in the spectra shape for pyrene solubilized in water or in copolymer solutions. This is illustrated in Figure 7 by the straight-line plots of F_0/F vs [I[−]] for pyrene in water and in the graft copolymers with various compositions. The ionic quencher I[−] that can readily quench pyrene in water had almost no effect on the intensity of the steady-state pyrene fluorescence in copolymer solutions. K_{SV} values of 93.4, 2.0, 1.7, and 0.9 M^{−1} were determined for pyrene in water and pyrene in aqueous solutions of copolymers 1, 2, and 3, respectively. Consequently, it can be concluded that each copolymer system had hydrophobic sites to restrict solute mobility, which inhibited the quencher–probe interaction. Repulsion between highly hydrated iodide ion and PNIPAm chains might be also responsible for the marked decrease in the accessibility of I[−] in the case of copolymer system. In addition, for

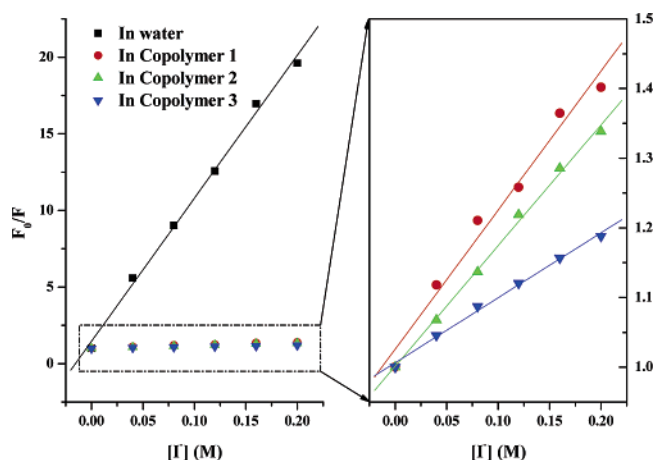


Figure 7. Quenching of pyrene by I[−] in aqueous copolymer solutions and water. [pyrene] = 6.0 × 10^{−6} M.

the copolymer with various compositions, K_{SV} was slightly decreased as EAB content was increased, indicating more compact hydrophobic domains were formed due to enhanced hydrophobic interaction between EAB groups for copolymer with higher EAB content. This was consistent with the above-mentioned morphology studies on copolymer aggregates. Different hydrophilic/hydrophobic balance of the copolymers led to various morphologies ranging from network to particles in aqueous solution, which means to establish microdomains with different hydrophobicity, and hence gave rise to distinct accessibility to ionic quencher. Similar result was reported for acrylamide–styrene block copolymers,¹⁷ where K_{SV} was decreased with an increase in hydrophobic styrene block length.

Conclusions

Both TEM and AFM observations indicated that the self-assembly morphologies of PNIPAm/EAB–PPPs were regulated along with the variation of copolymer composition which can be achieved due to the synthetic flexibility and versatility of polyphosphazene. On the other hand, depending on various solvents employed in aggregate preparation procedure, multimorphological assemblies ranging from network structure and nanospheres to high-genus particles were observed for the copolymer containing a relatively high EAB content. It seems a novel protocol to architecture supramolecular assemblies with multiple morphologies from graft copolymer. Also, the temperature would induce the morphology change of aggregates, which was resulted from the thermosensitivity of PNIPAm segments in the copolymers. These aggregates may find wide applica-

tions in pharmaceuticals, bioengineering and other related field as well.

Acknowledgment. Financial support from National Natural Science Foundation of China (No. 50203012) and Zhejiang Natural Science Foundation (No. R204233) is gratefully acknowledged.

Supporting Information Available: Text giving the synthetic method and characterization of amphiphilic graft copolymers and figures showing the FT IR and ^1H NMR spectra, temperature-dependent transmittance, and intensity ratios as a function of $\log C$. This material is available free of charge via the Internet at <http://pubs.acs.org>.

References and Notes

- (1) (a) Zhang, L.; Eisenberg, A. *Science* **1995**, *268*, 1728. (b) Discher, B. M.; Won, Y.-Y.; Ege, D. S.; Lee, J. C.-M.; Bates, F. S.; Discher, D. E.; Hammer, D. A. *Science* **1999**, *284*, 1143. (c) Riess, G. *Prog. Polym. Sci.* **2003**, *28*, 1107. (d) Bates, F. S.; Jain, S. *Science* **2003**, *300*, 460. (e) Jenekhe, S. A.; Chen, X. L. *Science* **1998**, *279*, 1903.
- (2) (a) Won, Y.-Y.; Davis, H. T.; Bates, F. S. *Science* **1999**, *283*, 960. (b) Antonietti, M.; Förster, S. *Adv. Mater.* **2003**, *15*, 1323.
- (3) Graff, A.; Sauer, P.; van Gelder, P.; Meier, M. *Proc. Natl. Acad. Sci. U.S.A.* **2002**, *99*, 5604.
- (4) Nardin, C.; Widmer, M.; Winterhalter, M.; Meier, M. *Eur. Phys. J. E* **2001**, *4*, 403.
- (5) Bae, Y.; Fukushima, S.; Harada, A.; Kataoka, K. *Angew. Chem. Int. Ed.* **2003**, *42*, 4640.
- (6) Chiu, D. T.; Wilson, C. F.; Karlson, A.; Danielson, A.; Lundqvist, A.; Stroemberg, F.; Ryttsen, M.; Davidson, F.; Nordholm, S.; Orwar, O.; Zare, R. N. *Chem. Phys.* **1999**, *247*, 133.
- (7) (a) Liu, F.; Eisenberg, A. *J. Am. Chem. Soc.* **2003**, *125*, 15059. (b) Soo, P. L.; Eisenberg, A. *J. Polym. Sci., Part B: Polym. Phys.* **2004**, *42*, 923. (c) Spatz, J. P.; Sheiko, S.; Möller, M. *Macromolecules* **1996**, *29*, 3220. (d) Ding, J.; Liu, G. *Macromolecules* **1997**, *30*, 655. (e) Cornelissen, J. J. L. M.; Fischer, M.; Sommerdijk, N. A. J. M.; Nolte, R. J. M. *Science* **1998**, *280*, 1427. (f) Stoenescu, R.; Meier, W. *Chem. Commun.* **2002**, 3016. (g) Wang, H.; Wang, H. H.; Urban, V. S.; Littrell, K. C.; Thiagarajan, P.; Yu, L. *J. Am. Chem. Soc.* **2000**, *122*, 6855. (h) Rodríguez-Hernández, J.; Lecommandoux, S. *J. Am. Chem. Soc.* **2005**, *127*, 2026.
- (8) Ilhan, F.; Galow, T. H.; Gray, M.; Clavier, G.; Rotello, V. M. *J. Am. Chem. Soc.* **2000**, *122*, 5895.
- (9) (a) van Hest, J. C. M.; Delnoye, D. A. P.; Barrs, M. W. P. L.; van Genderen, M. H. P.; Meijer, E. W. *Science* **1995**, *268*, 1592. (b) Yan, D.; Zhou, Y.; Hou, J. *Science* **2004**, *303*, 65. (c) Zhou, Y.; Yan, D. *Angew. Chem. Int. Ed.* **2004**, *43*, 4896. (d) Schappacher, M.; Putaux, J. L.; Lefebvre, C.; Deffieux, A. *J. Am. Chem. Soc.* **2005**, *127*, 2990.
- (10) Zhang, J. X.; Qiu, L. Y.; Jin, Y.; Zhu, K. J. *Colloids Surf. B-Biointerfaces* **2005**, *43*, 123.
- (11) Lehrer, S. S. *Biochemistry* **1971**, *10*, 3254.
- (12) (a) Zhang, L.; Eisenberg, A. *J. Am. Chem. Soc.* **1996**, *118*, 3168. (b) Soo, L. P.; Eisenberg, A. *J. Polym. Sci.: Part B: Polym. Phys.* **2004**, *42*, 923.
- (13) (a) Xu, R.; Winnik, M. A. *Macromolecules* **1991**, *24*, 87. (b) Wilhelm, M.; Zhao, C. L.; Wang, Y.; Xu, R.; Winnik, M. A. *Macromolecules* **1991**, *24*, 1033. (c) Gao, Z.; Desjardins, A.; Eisenberg, A. *Macromolecules* **1992**, *25*, 1300. (d) Zhang, L.; Barlow, R. J.; Eisenberg, A. *Macromolecules* **1995**, *28*, 6055. (e) Lin, Y.; Alexandridis, P. *J. Phys. Chem. B* **2002**, *106*, 10845. (f) Sakuma, S.; Hayashi, M.; Akashi, M. *Adv. Drug. Deliv. Rev.* **2001**, *47*, 21. (g) Wu, Y.; Zheng, Y.; Yang, W.; Wang, C.; Hu, J.; Fu, S. *Carbohydr. Polym.* **2005**, *59*, 165. (h) Carrot, G.; Hilborn, J.; Knauss, D. M. *Polymer* **1997**, *38*, 6401.
- (14) (a) Döbereiner, H.-G. In *Giant Vesicles*; Luisi, P. L., Walde, P., Eds.; John Wiley & Sons: New York, 2000; p 150. (b) Haluska, C. K.; Gozdz, W. T.; Döbereiner, H. G.; Förster, S.; Gompper, G. *Phys. Rev. Lett.* **2002**, *89* (23), 238302.
- (15) Qiu, L. Y.; Zhang, J. X.; Jin, Y.; Zhu, K. J. *Chin. Sci. Bull.* **2005**, *50*, 1453.
- (16) Zhang, L.; Eisenberg, A. *J. Am. Chem. Soc.* **1996**, *118*, 3168.
- (17) Dowling, K. C.; Thomas, J. K. *Macromolecules* **1990**, *23*, 1059.

MA052152Q